

Backscattering of ballistic electrons in a corrugated-gate quantum wire

Y. Ochiai, A. W. Widjaja, N. Sasaki, and K. Yamamoto

Department of Materials Science, Chiba University, 1-33 Yayoi-cho, Inage-ku, Chiba 263, Japan

R. Akis and D. K. Ferry

Nanostructures Research Group, Center for Solid State Electronics, Arizona State University, Tempe, Arizona 85287-6206

J. P. Bird, K. Ishibashi, Y. Aoyagi, and T. Sugano

Nanoelectronics Materials Laboratory, Frontier Research Program, RIKEN, 2-1 Hirowawa, Wako, Saitama 351-01, Japan

(Received 23 December 1996; revised manuscript received 24 February 1997)

We observe periodic oscillations in the weak magnetic-field magnetoresistance for quantum wires subjected to a corrugated gate. This enhanced magnetoresistance is attributed to backscattering of electrons from the gate corrugations due to direct ballistic trajectories through the multiple (open) quantum dot structures. Simulations of the quantum transport also show evidence of the enhanced magnetoresistance, suggesting that the classical backscattering trajectories are carried into the quantum behavior of the wire. [S0163-1829(97)02127-9]

It has long been known that the electrical properties of mesoscopic semiconductor structures are strongly influenced by the phase-coherent nature of the electron waves. One of the best known examples is the concept of weak localization. In diffusive systems, weak localization is caused by coherent backscattering from the diffusive impurity scattering centers, in which time-reversed paths lead to phase interference and enhanced resistivity at a zero magnetic field.¹ By breaking time-reversal symmetry, a small magnetic field destroys the interference of the paths and dramatically damps the enhanced resistivity. Weak localization has also been observed in ballistic quantum dots, in which the mean free path is larger than the dot dimension. Hence, scattering occurs primarily from the potential walls of the confining barriers, and weak localization has been attributed to chaotic behavior within the quantum dot.^{2,3} However, it has recently been observed that weak localization can be observed in structures defined simply by two quantum point contacts,^{4,5} so that there is no possibility of chaotic transport. Rather, it was conjectured by these authors that ballistic electrons could be reflected from the edges of the quantum point contacts, in a manner such that time-reversed orbits arose, and that this led to the weak localization. In agreement with this, it has also been shown that scattering off one or two impurities can lead to weak localization in a single quantum point contact,⁶ a view in strong contrast to the normal invocation of chaos for weak localization. This suggests that the appearance of weak-localization-like behavior can arise merely from ballistic backscattering orbits, in a manner in which phase interference can arise, such as reflection in triangular dots.⁷ Consequently, it is of interest to see if other magnetoresistance peaks, at nonzero magnetic field, can similarly be related to classical backscattering processes.

While it is difficult to probe directly the nature of the time-reversed paths at zero magnetic field, it is possible to study the enhanced resistance that can arise from phase interference of backscattered electrons in a finite magnetic field. Here, we report on the nature of the enhanced magnetoresistance in quantum wires in which the lateral gate is

corrugated so as to induce a series of coupled (but open) quantum dots in the wire. We observed enhanced resistivity at those magnetic fields for which selected orbits are backscattered from the corrugations, thus causing a reduction in the transmission coefficient at the entrance quantum point contact.

The dot array samples were fabricated on a high mobility GaAs/Al_xGa_{1-x}As heterojunction wafer. The samples are first mesa isolated and then the lateral gates are patterned using electron-beam lithography and liftoff of the Ti/Au metallization. The resultant gates are sketched in Fig. 1, and the corresponding dimensions of the wire and the corrugations are indicated there. At 0.6 K, the ungated carrier density of the two-dimensional (2D) electron gas is $2.7 \times 10^{11} \text{ cm}^{-2}$ and the Hall mobility is $480\,000 \text{ cm}^2/\text{V s}$. A negative bias of -0.5 V is sufficient to deplete the carriers under the lateral gates thus forming the quantum wire. For sufficiently negative bias, the wire can be narrowed to a coupled dot array. Measurements to be discussed here are made in the (open) quantum wire regime, and over the range of gate biases discussed below, we estimate that 2–12 modes are present in the wire. While the quantum point contact can be expected to collimate the beam,⁸ the symmetry of the point contacts here

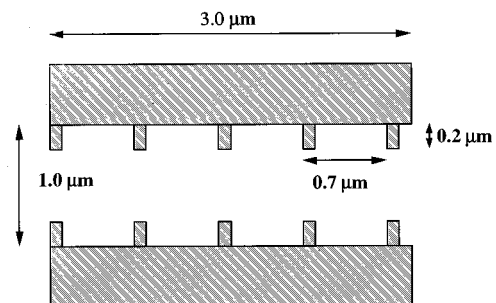


FIG. 1. The schematic diagram of the depletion gates is shown here. The corrugations induce a similar corrugation upon the electron gas, but the actual size of the potential will depend upon the details of the self-consistent fields in the channel.

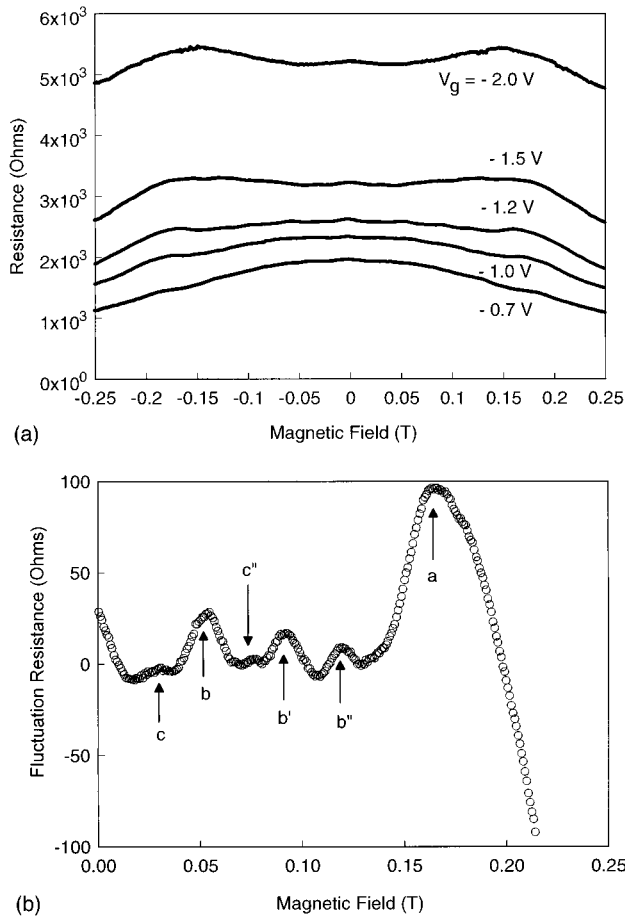


FIG. 2. (a) The magnetoresistance is shown for a range of gate voltages. The more negative voltages cause a narrower channel through the point contacts formed by the corrugations. (b) An expanded view of the oscillatory part of the conductance for the case of $V_g = -1.2$ V.

should lead to the majority of injected carriers being directed directly down the quantum wire. Current-biased measurements were performed utilizing a four-probe configuration with two lock-in amplifiers. The bias current in the sample is kept sufficiently low so that the bias across the sample is kept below $1 \mu\text{V}$. The mean free path of the carriers is estimated to be more than $4 \mu\text{m}$, which is considerably larger than the dimensions of the wire, and we estimate that the wire is in the quasiballistic limit, with little scattering from within the wire itself.

In Fig. 2(a), we plot the magnetoresistance of the wire at several values of the gate bias. In each case, there is a clear weak-localization peak at zero magnetic field, and a strong general negative magnetoresistance that persists to beyond 0.2 T. This latter is felt to be due to the general enhanced coupling to the wire at the input contact that arises as the 2D electrons undergo less back scattering from the entrance at higher magnetic fields.¹ Superimposed upon the general negative magnetoresistance is a series of additional peaks with the most prominent occurring in the range 0.05–0.2 T at each gate voltage. These peaks occur in each trace, but are most pronounced in the trace for $V_g = -1.2$ V. We have subtracted the background magnetoresistance and plotted just the peak structure in Figs. 2(b) for this latter trace. These

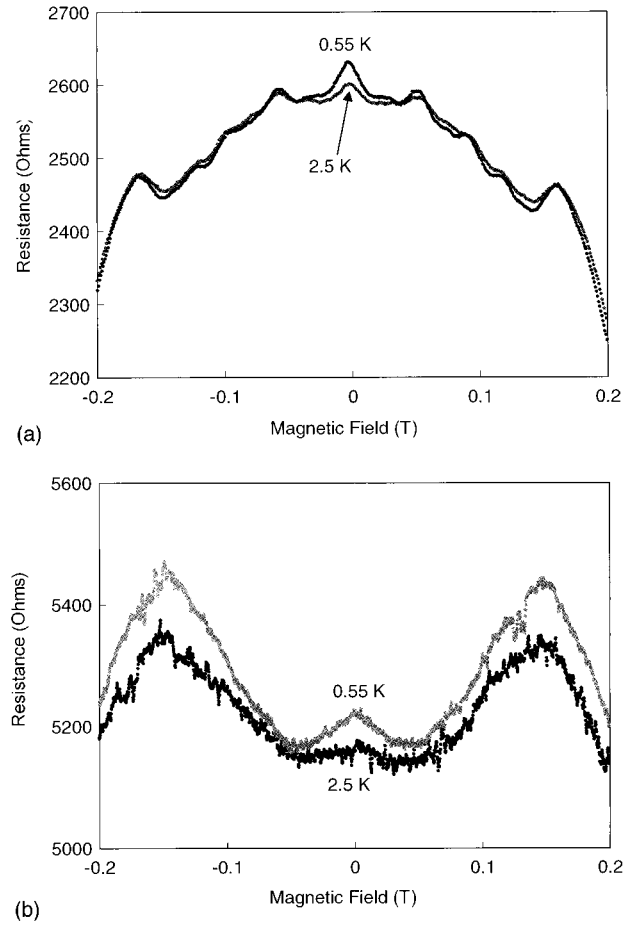


FIG. 3. The effect of temperature is only weakly observed on the oscillatory parts of the conductance, but is a big effect on the weak localization. In (a) the data are shown for $V_g = -1.2$ V, while in (b) the data are shown for -2.0 V.

peaks have been labeled a , b , b' , b'' , c , and c'' in this figure. It is important to note that these peaks do not occur in a wire in which only one side is given the corrugation.⁹ Hence, it may be concluded that these peaks arise from processes which involve both corrugations themselves in a fundamental way. Backscattering from the corrugations is such a process.

It is commonly observed that quantum interference is generally accompanied by a very strong temperature dependence. In Fig. 3, we show two magnetoresistance traces obtained at different temperatures, and for two different gate voltages. From this, it may be seen that the central peak at $B=0$ is very rapidly damped with temperature, reinforcing the observation that this is likely a phase-coherent weak localization. On the other hand, the backscattering peaks are only weakly damped in going to the higher temperature. This suggests that this is not a phase-coherent property, but is the result of semiclassical orbits reflecting and backscattering into the input quantum point contact.

With the gate bias applied, the actual potential profiles are not those indicated from the metallization of Fig. 1. Rather, there is edge depletion around the gates and this leads to noticeable rounding of the corrugations, both at the tips and at the point where they join the gate proper. Consequently, it is possible for carriers to be deflected by the magnetic field

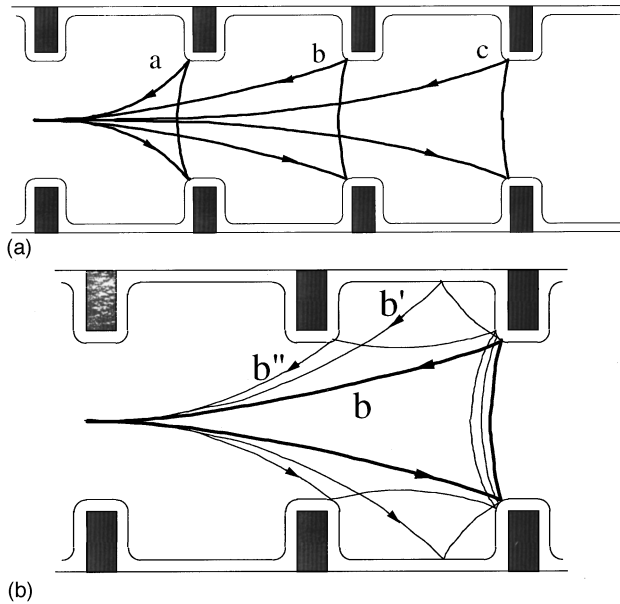


FIG. 4. (a) The conceptual source of the magnetic-field-induced backscattering orbits that lead to enhanced resistance is sketched here. (b) More complicated orbits are thought to give rise to extra resistance peaks.

so that they strike the corrugation, are reflected across the wire to the other side, and then so deflected that they arise back at the entrance point contact. In Fig. 4(a), suggested orbits for peaks a , b , and c are indicated schematically. These three peaks correspond to transit through one, two, and three dot regions before back reflection. Peaks b' and b'' are thought to be variants of orbit b , and these are shown in Fig. 4(b). *It must be emphasized, however, that these orbits are only suggestive, and we will deal with actual simulated orbits below.* Obviously, with such an open structure, many other orbits than the ones shown in the figure can be conceived. However, the orbits that we have used in this figure have the important property that their *symmetric* nature allows for the particles to be backscattered all the way from one end of the structure through a few dots and back to the entry contact. Such orbits cannot occur in a single-sided corrugation which, as we have mentioned, does not show the backscattering peaks.

Enhanced resistance at a given magnetic field arises from a reduction in the transmission through the wire, and this reduction is due to the onset of the backscattering process, whether quantum or classical.^{10,11} The backscattering here is unlikely to be due to phase coherence within the loop, although this may play a part in the amplitude of the enhanced resistance, as will be discussed below. This is reinforced by its weak temperature dependences, in contrast to the strong temperature damping observed in the weak localization (and phase-coherent peak). Rather, it is likely to be due to simply the reduction in transmission caused by the backscattering process. Nevertheless, this process, and the classical orbits that result, carry over to a quantum-mechanical treatment of the transport. We have carried out a simulation of the corrugated quantum wire using a stabilized variant of the lattice transfer-matrix approach.^{8,12} The experimental data and a calculated conductance curve are shown in Fig. 5. The latter has been smoothed to correspond to the finite temperature of

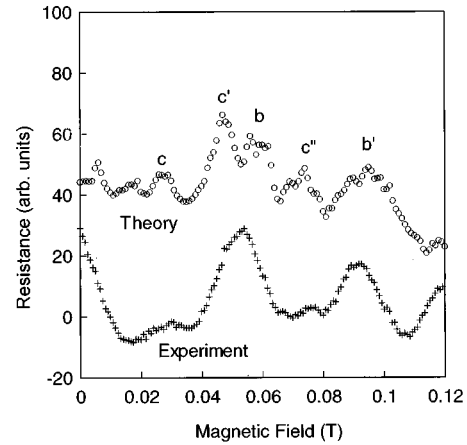


FIG. 5. Comparison of the theoretically calculated resistance fluctuations and the experimentally observed fluctuations. The single peak near 55 mT in the experiment seems to be two closely spaced peaks at 47 and 58 mT.

the experiment. It is clear that the quantum calculation shows enhanced resistance at peaks corresponding to those observed in the experiment. The theory, however, suggests that the peak at about 50–55 mT is actually composed of two contributions, the previously designated b (58 mT), and the missing c' (47 mT). This gives rise to the rather broad single peak seen in the experiment. It should be noted that the rounding of the potential, both in the corners of the “dots” and at the peaks of the corrugations, is crucial to provide the proper angle for reflection that gives rise to the backscattering peaks. This rounding is a natural result of the self-consistent potential in the wire. The simulations are consistent with the idea that corrugation shape is crucial in determining the backscattering orbits. We obtain qualitatively similar results using different degrees of rounding, but the position of the peaks is highly dependent on the shape. Even small changes in the shape of the corrugation tips can make a significant difference.

While the backscattering arises from specific semiclassical trajectories, it is clear that these are replicated in the quantum-mechanical simulation of the wire, and strongly affect the wave functions themselves. In Fig. 6, we plot the results of classical billiard simulations and those of the quantum simulation for comparison for a field of 22 mT (peak c). Only the backscattered trajectories are plotted for the classical case. Panel (a) shows the classical backscattered trajectories in all four dots, while (b) enhances just the last two dots. For comparison, we plot the quantum simulation results in (c). It is clear that the regions of high probability density (dark areas) correspond to the regions of large numbers of backscattered trajectories. We must remember that this is an open system and the “resonances” in the wave function must arise from the backscattering processes. A similar behavior is seen at each of the other peaks. While it is clear that there is a great deal of similarity in the classical and quantum simulations, it is just as clear that the conceptual orbits of Fig. 4 are quite simplified, although they convey the generic idea of the backscattering processes. More detail will be published elsewhere.

In summary, we have observed enhanced magnetoresistance peaks which are clearly connected with ballistic back-

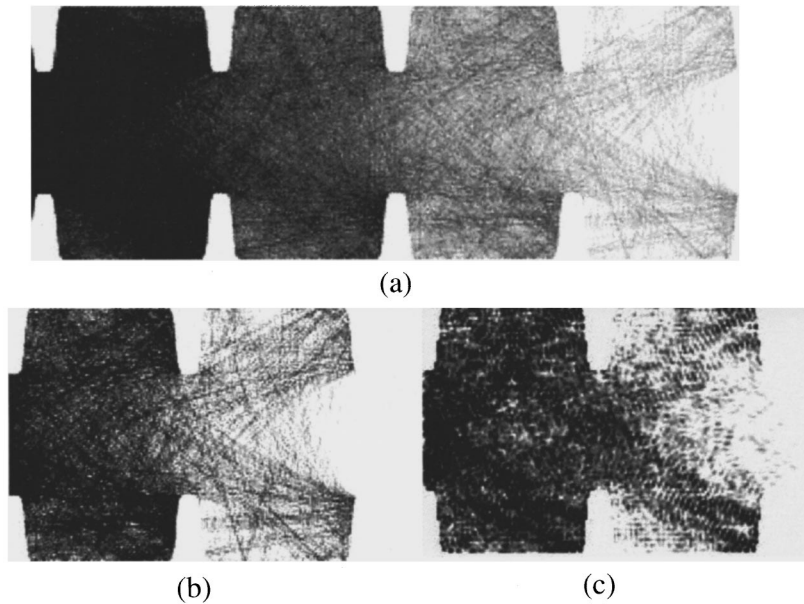


FIG. 6. Results of classical and quantum simulations. (a) The backscattering trajectories for the classical particle injected at the left-hand side of the structure for 22 mT. (b) Enhancement of the last two cells. (c) The quantum wave-function amplitude shows a behavior that suggests the carryover of the classical orbits into the quantum regime. This figure shows the wave function in the last two cells of the four cell structure.

scattering trajectories in the corrugated-gate quantum wire. The presence of the backscattering is clear evidence for the stability of classical orbits in the quantum structure that composes the wire, and the fact that these orbits are exceedingly sample specific. Moreover, the presence of the enhanced magnetoresistance in the quantum simulations is substantial support for the extension of the classical orbits into quantum contributions to the overall density of states of the system.¹³ Simulations of both the classical orbits and the quantum wave functions suggest a deeper connection to the enhanced magnetoresistance. Finally, the observation of these orbits and backscattering peaks is support for the existence of a weak-localizationlike behavior at zero magnetic field that is

caused by ballistic reflections from generic scattering edges in the quantum structures.

The authors would like to express their appreciation to Per Omling and Dragica Vasileska for many helpful discussions, and to the former for sharing results of their experiments prior to publication. Portions of this work were supported (Chiba U.) by a grant in aid for the Science Research Project on the priority area of “Single Electron Devices and Their High Density Integration” from the Ministry of Education, Science, and Culture of Japan, and (ASU) by the Office of Naval Research and the Defense Advanced Research Projects Agency.

¹C. W. J. Beenakker and H. van Houten, in *Solid State Physics: Advances in Research and Applications*, edited by H. Ehrenreich and D. Turnbull (Academic, New York, 1991), Vol. 44, pp. 1–228.

²H. U. Baranger, R. A. Jalabert, and A. D. Stone, *Phys. Rev. Lett.* **70**, 3876 (1993).

³J. P. Bird, D. M. Olatona, R. Newbury, R. P. Taylor, K. Ishibashi, M. Stopa, Y. Aoyagi, T. Sugano, and Y. Ochiai, *Phys. Rev. B* **52**, 14 336 (1995).

⁴R. P. Taylor, R. Newbury, R. B. Dunford, P. T. Coleridge, A. S. Sachrajda, and J. A. Adams, *Phys. Rev. B* **51**, 9801 (1995).

⁵J. A. Katine, M. A. Eriksson, R. M. Westervelt, K. L. Campman, and A. C. Gossard, *Superlattices Microstruct.* **20**, 337 (1996).

⁶A. Grincwajg, G. Edwards, and D. K. Ferry, *Physica B* **227**, 54 (1996); A. Grincwajg and D. K. Ferry, *Phys. Rev. B* **55**, 7680

(1996).

⁷P. Omling, H. Linke, L. Christensson, and P. E. Lindelof, *Jpn. J. Appl. Phys.* (to be published).

⁸R. Akis, D. K. Ferry, and J. P. Bird, *Phys. Rev. B* **54**, 17 705 (1996).

⁹W. Widjaja, N. Sasaki, K. Yamamoto, Y. Ochiai, J. P. Bird, K. Ishibashi, Y. Aoyagi, T. Sugano, and D. K. Ferry, *Superlattices Microstruct.* **20**, 317 (1996).

¹⁰R. Landauer, *IBM J. Res. Dev.* **1**, 223 (1957).

¹¹J. McKelvey, R. L. Longini, and T. P. Brody, *Phys. Rev.* **123**, 51 (1961).

¹²T. Usuki, M. Saito, M. Takatsu, R. A. Kiehl, and N. Yokoyama, *Phys. Rev. B* **52**, 8244 (1995).

¹³M. V. Berry and K. E. Mount, *Rep. Prog. Phys.* **35**, 315 (1972).